A Comparison of FGGE Wind Observations in the Tropics with General Circulation Model Similarities

A REPORT

from the space science and engineering center
the university of wisconsin-madison
madison, wisconsin

A Comparison of FGGE Wind Observations in the Tropics with General Circulation Model Similarities

Final Project Report

to

National Aeronautics and Space Agency
Grant NAG 5-301
1 April 1983 to 31 March 1984

from

The Space Science and Engineering Center
of the University of Wisconsin-Madison
1225 West Dayton Street
Madison, Wisconsin 53706

Verner E. Suomi
Principal Investigator

Donald P. Wylie
Co-Investigator

October 1984

Table of Contents

Abstract

Low level cloud motions and merchant ship wind observations from the GWE were analyzed on 2°x 2° latitude and longitude grids for estimating the wind stress on the oceans in the tropics (NSF program). The separate wind field analyses from cloud and ship data were compared to the wind fields from the lowest level of the GLAS model (940 mb). Two monthly averages were made for January and February 1979. Good agreement was found between the cloud motion and model fields. The ship fields, however, had large gaps and appeared to be internally noisy when compared to the other fields. The three monthly averaged fields were highly correlated, with coefficients ranging from 0.82 to 0.95. The mean biases were under 1.4 m/s, and grid point root mean squared differences were less than 1.5 m/s.

Autocorrelation and variance statistics were calculated for seven types of wind data in the western hemisphere tropics. Six of these data sets came from the Global Weather Experiment (GWE) in January 1979. They were: 1) cloud motion measurements from four different sources, 2) radiosonde wind reports, 3) synoptic land station reports, 4) marine ship reports, 5) aircraft pilot reports, 6) automatic aircraft reports for the GWE. The seventh data set consisted of Seasat scatterometer winds from September 1978. Winds were analyzed within a target area from 30°N to 30°S latitude and 0° to 180°W longitude.

The Seasat scatterometer data had the best auto-correlations and lowest standard deviations. Cloud motion and radiosonde had lower auto-correlations than Seasat. Synoptic land stations, ship reports, and aircraft pilot reports had noticeably poorer auto-correlations, implying higher internal noise levels or sensitivity to small scale fluctuations. Structure function plots of autocovariances against distance between observations indicated that Seasat was most sensitive to wind field structure. The structure function plots for other low level wind observations indicated a lack of structure sensitivity for scalar wind speeds. All observations, however, were sensitive to structure in the wind direction patterns.

1. Introduction

The objective of this grant was to evaluate how wind observations are used in general circulation numerical models and to improve their use in these models. This objective stems from the involvement of the University of Wisconsin-Madison in the Global Atmospheric Research Program First Global Experiment (FGGE, also called the Global Weather Experiment or GWE) as a producer of wind observations. This project was a logical follow-up to the FGGE experiment and an attempt to improve data gathering efforts in the future.

The project concentrated on two areas: 1) a comparison of gridded analyses of winds to the wind fields resident in a model, and 2) the statistical properties of wind data obtained from different observing systems. Two months of model simulations from 5 January to 28 February in 1979 made by NASA's Goddard Laboratory for Atmospheric Sciences (GLAS) were compared to analyses of the low level cloud motions and also ship reports over the oceans made at Wisconsin. These comparisons are summarized in Section 2 of this report.

Section 3 discusses properties of wind data from several different sources. Emphasis is placed on autocorrelation and variance statistics.

General circulation models have to form a composite representation of the atmosphere using all the observations that are available. These data have to be edited and smoothed to eliminate the bad or noisy observations. The weighting functions used for averaging and smoothing data should be based on the characteristics of the data themselves, the characteristics of the atmosphere, and the desired degree of detail or smoothness. The autocorrelation and covariance statistics were compiled to aid in the design of methods for ingesting these data into the models. These statistics have been compiled into a manuscript submitted to the Monthly Weather Review (journal sponsored by the American Meteorological Society) for publication.

2. Comparisons of Monthly Averaged Wind Fields from Cloud Motion Observations, Ship Reports, and GLAS Model Simulations

2.1 Overview of Comparisons

Three sources of wind data were originally analyzed for an NSF sponsored program on wind stress over the oceans. We compared these analyses to the GLAS model simulations to see if there were any major differences between analyses purely from wind data with no "physics" and the model's depiction of the same field.

The method used for assimilating wind data into the model and forming wind fields is described in Baker (1983). Much more data are used in the model than the cloud motion and ship reports examined here. The model requires the mass field and velocity field to exhibit an appropriate degree of balance in each of the vertical layers according to physical principles. The mass field is obtained, for the most part, from sounding data independent of the data used here for wind analyses. Thus, in contrast to this elaborate method of analyzing data which is necessary for running forecast models, we were compiling simple analyses from single data sources. Comparisons among these three depictions of the wind field gives an indication of our ability to consistently represent tropical wind fields and reveals some deficiencies in the sources of the data.

2.2 Data Sets Used

The low level cloud motions from five geostationary satellites were used. These were produced by NOAA/NESS and the University of Wisconsin for the GOES-East and West satellites in the Western Hemisphere, 20°W to 180°W longitude. In the eastern Atlantic and western Indian oceans, cloud motions were extracted from Meteosat images by the European Space Agency. The western Pacific was coverd by the Geostationary Meteorological Satellite (GMS) from which cloud motions were extracted by the Japanese Meteorological Agency and also the University of Wisconsin. The Indian Ocean was covered by a third geostationary satellite from the GOES series of the United States. Redundant analyses were made on the GOES-East and West and GMS imagery by the University of Wisconsin.

Only low level cloud motions were used for the wind analyses. All observations between 700 mb (800 mb for Wisconsin observations) and the surface were summarily grouped into this category. More detailed height categorizations were not attempted because of two factors: (1) Most low level clouds move with the speeds of their bases, not their tops (Hasler et al. 1979), and their motions are not "point" observations in the vertical for which precise heights can be designed. (2) Various analysis centers (and sometimes analysts within a given center) assigned heights differently. Some used the cloud top height inferred from infrared measurements of the cloud top (JMA and ESA), while others assigned all low level clouds to cloud base estimates (Wisconsin) or the level of a statistical "best fit" when compared to radiosonde data which were determined to be 900 mb by NOAA/NESS.

With this confusion, which is attributable partly to physical reality as well as political preference, we chose to use a broad layer categorization in which most cloud motions reported below 700 mb represent "low level" winds. This fit the data gathering tendencies since most cloud motions were either in this low level range or in a high level range from 100-300 mb with very few cases of more than one vertical category observable at the same horizontal location. As mentioned above, the Wisconsin low level height category was restricted to heights below the 800 mb surface. By standard practice at Wisconsin, occasional cloud motions reported from 700-800 mb were intended to be middle atmosphere clouds and not low level boundary layer influenced clouds.

The wind analyses considered here are restricted to ocean areas since these analyses were made by another program for the estimation of wind stress on the ocean. The analyses were made on a daily basis, using the cloud motion data close to local noon on each day. The Wisconsin coverage of GOES-East and West was also limited to ±15° latitude, while the other producers and Wisconsin products covered the full viewing areas of each satellite which was 50° from the satellite's subpoint.

Observations were averaged at grid points, using a distance weighting function

$$w = 4/(4+R^2) \qquad (2.1)$$

where R is the distance in degrees of latitude and longitude. Only observations within 6° of each grid point were used. Where less than two observations within a 6° radius were found, the grid point was left unfilled for that day. The ship analyses had many unfilled grid points due to concentration of data along major ship routes and the resulting dearth in other areas.

Data quality checks were made on the observations. Any observations which disagreed with the average of the others used for a grid point by more than 5.0 m/s in the zonal (U) or meridional (V) components was rejected. This caused the rejection of many ship observations in the eastern Pacific along the western coast of Baja, Mexico. Even though this is a heavily travelled shipping lane, it is also an area of highly variant winds.

The daily grids for cloud motions and ship observations were averaged over the months of January and February. Grid points were not filled in the monthly average if more than 40% of the daily values also were missing. The GLAS model wind fields were archived at six-hour intervals on 4° latitude by 5° longitude grids. All model fields from 5-31 January were used for the January average plot, while all grids from 1-28 February were averaged for the following month.

2.3 Discussion

2.3.a. Graphical similarities

The most obvious feature, comparing the three wind fields (Figs. 2.1 and 2.2), is the absence of ship coverage in the Pacific Ocean. The ship coverage was only 68% of the cloud motion coverage over the oceans. The cloud motion wind fields closely agree with the model fields in most analyses, while the ship fields deviate from the other two, especially along the boundaries of data voids away from the shipping lanes.

The northeasterly trade winds in the northern hemisphere exhibit generally close agreement with the cloud motions and GLAS model. Jets or maxima in the Pacific and Atlantic of 6 to 10 m/s magnitude appear in both months in both analyses. The ship analyses underestimate the 10 m/s area in the Pacific and the 6 to 8 m/s area in the Atlantic.

Small differences can be found between the GLAS model and cloud motions. The northeast trades in the north Atlantic are stronger in the GLAS model in January (8 m/s) than the cloud motion or ship analyses which view around 6 m/s maximum. In February, the three analyses were more in agreement at 8 m/s, although the cloud motions show a larger area for the 8 m/s contour. Similar larger contour areas also appeared in the Pacific for the cloud motions in both months. Cloud motions 1-2 m/s faster than ship winds or the model 944 mb analyses, should be expected since the cloud data represent a higher level in the atmosphere.

The northeasterly winds of the winter monsoon agreed in all three analyses with a 6 m/s maximum along the east African coast for both months. Some disagreements were found on the equator and in the southern hemisphere. A small 10 m/s contour appears on the equator at 140°W on the cloud analysis in January and does not appear in the model field. Most of the central and southern Pacific is dominated by an 8 m/s contour on the cloud field, while the model has a 6 m/s contour. This difference was also present in February, but the small 10 m/s contour did not appear in the cloud field.

In the southern Atlantic, the southwesterly winds converging onto the Ivory Coast of Africa are more obvious in the ship fields than the model for both months, mainly due to the westerly directions along the coast. The cloud fields lack data in this area. The southeasterly trades in the southern Indian Ocean are stronger in the model than either the cloud motion or ship analyses. Small areas of 8 m/s appear in the model in both months, while the ship and cloud fields only have 6 m/s contours.

A similar difference appeared in the western Pacific in January at 8°S and 170°E where the model has a 10 m/s contour of northwesterly winds, while the ship and cloud fields have only 4-6 m/s contours. Directional patterns, although complicated in this area, are surprisingly similar among all three fields.

2.3.b Statistical similarities

The three wind analyses were highly correlated (see Table 2.1). Correlation coefficients of the monthly mean wind components ranged from 0.82 to 0.94, with the U component correlations higher than the V component correlations.

The average differences between analyses were also small. Cloud motion analyses were 1.2 m/s more easterly in the U component than the ships (Table 2.2). This is a normal vertical shear that has been found in past cloud-surface wind comparisons. Similar differences of 1.4 m/s were found between cloud motions and the 944 mb model analyses. The model closely agreed with the ship analyses for both months within 0.2 m/s mean bias in the U component. The mean differences in the V components were very small between all of the analyses, less than 0.2 m/s. The winds in the tropical belt were mostly easterly and V components were highly variant between the oceans and the two hemispheres across the equator.

The root mean square differences of the grid point values also were small. They ranged from 1.0 to 1.6 m/s (rms) (see Table 2.3). The cloud-model difference was the greatest, while the cloud-ship and ship-model comparisons were closer (1.0 to 1.4 m/s). Cloud-ship comparisons were the smallest (1.0-1.2 m/s). It should be noted that cloud data differ from the model fields on an individual basis from 2.2 to 2.8 m/s (Baker 1983). Thus, the averaging of data to monthly analyses improves these differences to 57%.

Table 2.1: Correlation between monthly average wind components at grid points

	Cloud-Ship	Cloud-Model	Ship-Model
January			
U	0.92	0.91	0.94
V	0.85	0.83	0.90
February			
U		0.91	0.94
V		0.82	0.93

Table 2.2: Average mean differences between analyses

	Cloud-Ship	Cloud-Model	Ship-Model
January			
U	-1.2 m/s	1.4 m/s	-0.1 m/s
V	-0.2	0.1	-0.1
February			
U		1.5	-0.2
V		0.0	0.0

Table 2.3: Standard deviation of differences between analyses

	Cloud-Ship	Cloud-Model	Ship-Model
January			
ΔU	1.0 m/s	1.6 m/s	1.4 m/s
ΔV	1.2 m/2	1.4	1.2
February			
ΔU		1.4	1.1
ΔV		1.4	1.0

3. Autocorrelations of Wind Observatons

3.1. The Role of Spatial Autocorrelations in Analysis

In recent years analyses of synoptic scale wind fields for studies of atmospheric dynamics or the initialization of numerical models have used a variety of data types. Radiosonde observations, nearly the sole source of synoptic information aloft in the past, have been augmented by newer types of data such as cloud motions and aircraft reports. Objective analysis schemes have had to become more complicated to blend these data. These analysis schemes assign weights to each observation based on several factors, such as proximity to a grid point, density of the observations, and the noise in each observation. Thus, the weight is partly determined for each type of data from known or estimated statistical characteristics of the data source. Specifically, to design weighting functions we should know: 1) the shape of the spatial autocorrelation function for each data source, and 2) the internal noise level of each data source (Barnes, 1964). Although biases need to be considered, they are not the focus of the study presented here.

There have been several investigations of the autocorrelation characteristics of wind data in the past for various geographical areas and time periods. For example, radiosonde autocorrelations are extensively discussed in Steinitz et al. (1971), using data over the northern hemisphere tropics over a five-year period from 1958 to 1963. Cloud motions were analyzed by Wylie and Hinton (1981a and b) over the Indian Ocean during the summer monsoon of 1979, other cloud motion characteristics were studied by Hubert and Whitney (1971) and Hasler _et al_. (1979) in the Atlantic Ocean, and Halpern and Knox (1983) in the tropical Pacific Ocean. Ship reports were studied by Pierson _et al_. (1980) in the Gulf of Alaska. These studies also contain some comparisons between two types of data from which bias can be assessed. But the differences in autocorrelations reported by these studies may be partly due to the differences in the wind fields between tropical and higher latitudes, and partly due to differing observation systems.

To further assess the differences within wind measurement systems, we calculated autocorrelation statistics from seven different data sources. To include low latitudes and significant ocean areas, the location of the study area was the tropical western hemisphere, 30°N to 30°S latitude, 0°W to 180°W longitude (see Table 3.1). Coverage of each data type is concentrated in a subregion within this box (described in the next section and Table 3.1). Six of the data types came from the Global Weather Experiment in January 1979. The seventh type of data was the microwave scatterometer winds from the flight of Seasat in September 1978. Seasat data were included because they contain mesoscale resolution (100 km) over global areas not obtainable from the other sources. The scatterometer is of special interest as it is expected to be used in future wind analyses when it is available from a new satellite (see Wylie and Hinton 1984).

3.2 Data Sources

All data, except Seasat, were obtained from the National Climatic Center (NCC) of the National Oceanographic and Atmospheric Administration (NOAA) in Asheville, North Carolina. NCC is a distributor for the special archives established for GWE data. The synoptic land station reports and

Table 3.1. The Data Sources used for Auto-Correlation Statistics

Wind Producer	Average # of Winds per Day	Time Period	Longitude Covered
Low Level			
Land Stations	295	1-31 Jan 79	0-180° W
Ship Reports	264	1-31 Jan 79	0-180° W
850 mb Raobs	68	1-31 Jan 79	0-180° W
NESS Cld. Mot.	204	15-31 Jan 79	30°W-150°W
Wis. Cld. Mot.	738	21-31 Jan 79	30°W-150°W
ESA Cld. Mot.	56	1-31 Jan 79	50°W-90° E
GMS Cld. Mot.	86	1-31 Jan 79	90°E-170°E
Seasat scat.	2235	6-7 Sep 78 11-14 Sep 78	20°W-180°W
High Level			
ESA Cld. Mot.	106	1-31 Jan 79	50°W-90° E
GMS Cld. Mot.	94	1-31 Jan 79	90°E-170°E
NESS Cld. Mot.	81	15-31 Jan 79	30°W-150°W
Wis. Cld. Mot.	450	21-31 Jan 79	30°W-150°W
250 mb Raob	65	1-31 Jan 79	0° -180°W
Conv. Aireps	103	1-31 Jan 79	0° -180°W
FGGE Aireps	13	1-31 Jan 79	0° -180°W

radiosonde data were taken from the Level II-b archive tapes. Ship reports were obtained from both the II-b tapes and the Supplementary Surface Marine Data Archive of GWE. Only the 12 GMT observations were used for the land, ship, and radiosonde data. Cloud motion and aircraft data were obtained from supplementary archives of the GWE. No editing or corrections were made to any of the data used other than the gridding criteria discussed in section 2.2.

Cloud motions were measured by four operations during the GWE. The GOES East and West satellites were analyzed from 20°W to 150°W longitude and 50°N to 50°S latitude by NOAA's National Environmental Satellite Service (NESS). Three wind sets per day were made. The 12 and 18 GMT data were combined for statistical analyses. These times were close to noon at the sub-satellite coverage points. The 00 GMT wind set was ignored.

A special cloud motion analysis was made by the University of Wisconsin-Madison for a tropical belt from 15°N to 15°S latitude in the GOES East and West areas once each day near local noon (12 or 18 GMT). The coverage of this analysis was considerably more dense than NOAA/NESS operational analyses because cloud targets were selected by meteorologists (see Mosher 1981).

Other cloud motion data sets were from Meteosat of the European Space Agency (ESA) and the Geosynchronous Meteorological Satellite (GMS) of Japan. Note that the ESA data were not included in the work discussed in Section 2. Correlation and variance statistics were made from the 6 and 12 GMT data of Meteosat and the 00 to 6 GMT data of the GMS.

Aircraft data were broken into two categories: 1) the conventional reports which are voice-transmitted by the pilot to ARINC (Aeronautical Radio, Inc.), and 2) the automatically recorded data. The conventional

Aireps require a pilot to calculate winds from data on true airspeed and groundspeed. These are sometimes subject to large measurement or calculation errors and errors in coding. Since the advent of inertial navigation systems in aircraft, wind data has been automatically obtained. For GWE, a special communications and recording system was devised to collect the data directly from the inertial navigation systems (see Sparkman _et al_. 1981). The Aircraft Integrated Data System (AIDS) recorded wind observations specially for GWE on some aircraft, while others automatically transmitted data to NOAA by the Aircraft-to-Satellite Data Relay (ASDAR). We used all AIDS and ASDAR reports within 3 hours of 12 GMT on each day. Voice-transmitted pilot reports within 3 hours of 12 GMT were analyzed separately from the automatically recorded data.

Seasat scatterometer wind data were obtained from the Jet Propulsion Laboratory (JPL) of The California Institute of Technology for September 1978. Winds were derived from the radar scatterometer data at 100 km resolution, using the SASS-1 algorithm (Jones, _et al_., 1982). Wind directions were manually selected from four choices given by the SASS-1 algorithm (Wurtele, _et al_. 1982). The directional selections were made independently by two teams of meteorologists, one at JPL and a second at the Atmospheric Environmental Service of Canada. The teams resolved their differences at a joint meeting at JPL attended by one of the authors of this paper. The hand-drawn directional analyses considered not only the scatterometer data, but all other available wind data except cloud motions. However, the editors chose only the wind directions from the four possible vectors given by the SASS-1 algorithm at 100 km intervals within and along the 1200 km wide swath of the satellite. Wind speeds were not edited, but were left as defined by the scatterometer and SASS-1 algorithm.

The Seasat scatterometer covered a swath 1200 km wide along the satellite's orbit. However, there is an interorbit gap of equal width at the equator, due to limitations of the instrument. In seven hours, the scatterometer covered approximately one-half of the tropical oceans. No wind information was obtained over land. Four orbits from 20°W to 150°W were combined each day for correlation and variance computations.

3.3 The Statistics Calculated from the Data

Autocorrelations and auto-covariances were calculated by forming all possible pairs of observations of the same time, data type (satellite, radiosonde, ship report, etc.), and altitude. These pairs then were classified by their separation distance in 100 km bins. For each distance bin, sums of the zonal (ΣU) and meridional (ΣV) components, their squares (ΣU^2, ΣV^2) and cross products ($\Sigma U_i U_j$, $\Sigma V_i V_j$) were compiled. The auto-correlation for each bin C(d) was calculated for each wind component and the scalar wind speed.

$$C(d) = \frac{\frac{1}{N}\Sigma X_i X_j - \frac{1}{2N}\Sigma X_i \Sigma X_j}{\sqrt{\frac{1}{N}\Sigma X_i^2 - (\frac{1}{N}\Sigma X_i)^2}\sqrt{\frac{1}{N}\Sigma X_j^2 - (\frac{1}{N}\Sigma X_j)^2}} \qquad (3.1)$$

where X is the wind component, U, V, or the scalar speed, S, and N the number of comparison pairs in the bin. We include scalar speed calculations because certain wind data sources that may be used in the future will give scalar speed information without direction (Wylie and Hinton 1984).

A vector correlation between the two observations also was defined as

$$C_{vector} = \{1-[(1-C_u^2)S_u^2+(1-C_v^2)S_v^2]/(S_u^2+S_v^2)\}^{\frac{1}{2}} \qquad (3.2)$$

$$S_u^2 = \frac{1}{M}\Sigma U^2 - \left(\frac{1}{M}\Sigma U\right)^2 \quad (3.3)$$

where S is the standard deviation of wind component U or V, and M the number of component values in each distance bin. The vector correlation is a correlation between difference vectors for all pairs in the distance bin. The vector and scalar speed correlations together allow us to infer the relative importance of directional information over scalar speed data. This is less readily seen in the zonal and meridional wind component statistics. Thus, we present the vector correlation in place of individual U and V component correlations. Autocorrelations are square roots of auto-covariances normalized by the variances of the data sample as part of the calculations shown in (3.1), (3.2), and (3.3).

We will use the autocorrelations in the discussion of the data as indications of the errors or noise in the observations. Ideally, coincident observations at the same location and time should be perfectly correlated, C = 1.0. Since all observations have some errors in them and we exclude identical observations from our paired statistics (i = j excluded), the calculated autocorrelations were always less than 1.0. The observation pairs also had to be categorized into bins of separation distance for computing the statistics. We chose a scale length of 100 km for our bin size so all observations within 100 km were categorized as coincident pairs.

In the following discussion we use the magnitude of the autocorrelation in the first bin (0-100 km) to indicate of the noise or quality of the observation. Consequently, those observations sensitive to much smaller scales (i.e., "point" observations) will exhibit an apparent noise due to small scale fluctuations. If the data are intended to represent a larger area, as in modelling applications, for which one wants to filter out subgrid scale motions, it is appropriate to consider scales much smaller than 100 km as noise.

The standard deviation and direction difference profiles give further indication of observation noise levels and errors, or wind field structure definition. For proximate observations (the 0-100 km distance bin) of nearly perfect data, we would expect the S.D. to be nearly zero. The S.D. or direction difference is partly a quantification of the typical error associated with individual observations. On the other hand, an increase in S.D. and direction difference with separation is expected due to actual wind field gradients. The slope of this profile is an indication of wind field structure, or the inability to define structure if no slope is present. At large separations the standard deviation is nearly equal to the variance of the total data set without regard to distance. Direction differences will grow to a limit near 90° because the limit of an individual comparison is ±180°, the shortest distance around the compass.

We will present both the autocorrelation and standard deviation or direction difference statistics for each data set in the next section. The autocorrelation profiles show the fraction of the variance that is correlated and how it changes with distance.

The statistics mentioned were calculated for one time period on each day in the western hemisphere, 30°N to 30°S latitude. Spatial autocorrelations were averaged from 6 to 31 days, depending on the data density. For numerous observations such as cloud motions and Seasat scatterometer winds, reliable autocorrelations could be obtained from a few days of compilation. Values of autocorrelations and variances exhibited only small day-to-day changes, so we did not feel compelled to compute these for the full 31 days. For less dense data, the correlations and variances were averaged for one month to form stable statistics. The longitude bounds for the high density data sets were restricted to the areas viewed by the satellite as shown in Table 3.1.

The autocorrelation and standard deviations were computed at two levels in the atmosphere, low level or surface observations and upper troposphere or high level observations. For radiosondes, we used 850 mb to represent low level winds and 250 mb for the high level winds. Surface land stations were all considered low level regardless of station elevation. Cloud motion reports below 800 mb were considered low level winds, and those between 100 and 300 mb, high level winds. The cloud motion data between 800 and 300 mb were not used.

As discussed in Sec. 2, we chose broad categories for cloud motions because of the inaccuracies in assigning heights to the data and the variety of methods used to assign heights by the different wind producers. Heights are usually assigned based on the temperature of the cloud top, which sometimes includes infrared emissivity/transmitivity estimates. Studies by Hasler et al. (1979) have shown that the low level clouds move with the speeds of their bases. Unfortunately, base height cannot be directly measured from satellites. Some wind producers, such as the University of Wisconsin-Madison, estimated base height. Others simply assigned 900 mb to these clouds because they obtained highest correlations with radiosonde data at this level on the average (Hubert and Whitney, 1971). For more details see Mosher (1981).

Aircraft reports between 10 and 12 km (altimeter readings) were classified as high level data. Reports below 10 km were disregarded.

Generally, 10 to 12 km encompasses 200 to 300 mb levels. Thus, aircraft reports were more restricted than the cloud motions in altitude range.

3.4 Results and Discussion

3.4.a. Low level winds

The Seasat scatterometer winds had the highest vector auto-correlation of 0.96 for the less than 100 km bin. (See Table 3.2 and Fig. 3.1a.) Radiosonde 850 mb winds, ship reports, and cloud motions from NESS and Wisconsin had slightly lower vector correlations of around 0.73. It should be noted that the data densities of radiosonde and NESS cloud motion observations were less than the other data types. Thus the statistics could not be calculated for separation distance bins below 300 km. Land stations had a noticeably lower vector correlation (0.54) than the others. This is partly due to orographic and coastal influences at many of the stations.

In addition, these data have the character of point observations mentioned earlier.

The slopes of the vector autocorrelations are similar for most of the data types. Seasat, however, decreased with distance slightly faster than the others. This is a possible indication of greater sensitivity to mesoscale detail or a result of having data confined to rectangular swaths under the satellite's orbital track. In other computations, not presented here, it was found that the size of the area used for computing autocorrelation statistics had a slight influence on the autocorrelation values for distances greater than 700 km. This is an expected "window" or viewing area effect.

Land stations had a noticeably steep drop in the vector correlation with distance. Geographical influences and sensitivity to small scale fluctations were again a probable cause of this profile.

Table 3.2. Average Auto-Correlations and Standard Deviation for 100 km and 400 km Separation Between Winds in the Tropics, 30°N-30°S

Wind Producer	100 km Vector Corr.	100 km Speed S.D.	100 km Dir Delta	400 km Vector Corr.	400 km Speed S.D.	400 km Dir Delta
Low Level						
Land Stations	0.54	2.9 m/s	45°	0.29	3.1 m/s	56°
Ship Reports	0.71	3.3	28°	0.54	3.8	41°
850 mb Raobs	----	---	--	0.73	3.5	37°
NESS Cld. Mot.	----	---	--	0.73	3.2	19°
Wis. Cld. Mot.	0.76	2.3	16°	0.66	2.8	21°
ESA Cld. Mot.	----	---	--	0.69	3.7	13°
GMS Cld. Mot.	----	---	--	0.72	2.8	17°
Seasat scat.	0.96	1.1	9°	0.82	2.2	21°
High Level						
ESA Cld. Mot.	----	---	--	0.82	7.8	19°
GMS Cld. Mot.	----	---	--	0.82	6.3	23°
NESS Cld. Mot.	----	---	--	0.88	6.9	11°
Wis. Cld. Mot.	0.90	4.4	15°	0.72	6.5	28°
250 mb Raob	----	---	--	0.76	8.5	20°
Conv. Aireps	0.74	10.9	14°	0.52	15.1	20°
FGGE Aireps	----	---	--	0.51	8.4	23°

The scalar speed autocorrelations were slightly lower than the vector autocorrelations (see Fig. 3.1a and b). The highest Seasat correlation dropped from 0.96 vector to 0.93 scalar. Similar small differences were found for radiosonde winds and Wisconsin cloud motions. Large drops in the correlations, vector to scalar, of 0.1 or more were found for NESS cloud motions, ship reports, and land station observations. The differences between the different data types also were slightly larger for the scalar speed autocorrelations than the vector correlations, as evident in Fig. 3.1.

Wind direction differences showed the same ranking among data types (Fig. 3.1c). Seasat had the lowest differences (9°), while cloud motions from NESS and Wisconsin were slightly higher (16°-19°). Ship reports were noticeably higher (28°). Radiosondes had direction differences of 37° at 300 km, similar to ship reports at the same distance. Land stations had the highest direction differences, exceeding 45°.

For Seasat, the direction differences grew faster with distance than any of the other data types (61° in 1500 km). This may indicate a sensitivity to mesoscale wind patterns. Cloud motions, in contrast to Seasat, had lower distance growth profiles (16° to 48°), which may indicate a lack of sensitivity to direction changes. This may result from spatial smoothing in the cloud motions, which are derived from one hour averages of target motions, while all other data types were nearly instantaneous observations.

Scalar speed S.D. in the 0-100 km separation bin showed some of the same distinctions between data types, but to a lesser degree than the correlation and direction differences. Seasat had the lowest S.D., 1.1 m/s, followed by Wisconsin cloud motions at 2.3 m/s. Ship reports and radiosondes had the highest S.D., 3.3-3.6 m/s.

Another feature was that the standard deviations of speed approached constant values at 600 km for all of the data types examined. Little growth in speed S.D. from 100-600 km was found for any data except Seasat. Land stations and NESS cloud motions had nearly constant S.D.'s for all distances. Flat profiles indicate either no resolved structure in the wind field, or that the errors or noise level of the scalar speed data were of nearly the same magnitude as the structure in the wind field.

3.4.b High level winds

The high level winds showed different characteristics than low level winds (Fig. 3.3). NESS cloud motions had the highest vector autocorrelations. Radiosondes and Wisconsin cloud motions were slightly lower, while aircraft reports (both pilot and automatic) were even lower. Most vector correlations decreased with distance at about the same rate. Exceptions were the automatic aircraft reports and radiosonde observations which dropped faster than the others. Automatic aircraft report correlations dropped to extremely small values at 600 km.

Trends in the scalar speed correlations were similar to the vector correlations, but at slightly lower values for most data types as was found for the low level winds. The exceptions were radiosonde 250 mb winds and aircraft pilot reports. For these the scalar speed correlations were slightly higher than the vector correlations out to 500 km. Two data types, the radiosondes and NESS cloud motions, had distinctively higher scalar speed correlations than the others out to 500 km. The aircraft reports (both pilot and automatic) and Wisconsin cloud motions had similar correlations out to 300 km, less than the radiosondes and NESS cloud motions.

The wind direction differences showed similar profiles for all the data types. They all increased with distance at approximately the same rate. NESS cloud motions had the smallest directional differences, while Wisconsin had the largest.

Scalar speed standard deviations increased with distance out to 900 km. The high level speed S.D. profiles indicated relatively more large-scale structure than the low level speed S.D. profiles which were nearly constant with distance.

The pilot reports had much higher speed S.D.'s than the other wind data. Wisconsin cloud motions were the lowest, with 4.4 m/s S.D. at 100 km, increasing to 7.8 m/s at 1000 km. Radiosondes ranged from 9.3 m/s S.D. at 300 km to 13.5 m/s at 1200 km, with NESS cloud motions and automatic pilot reports falling between the Wisconsin cloud motions and radiosonde data. The pilot reports were in a class by themselves, much higher than the others, ranging from 10.9 m/s S.D. at 100 km to 17 m/s at 1200 km.

3.4.c Comparison of cloud motions from different producers

Statistics from four cloud motion producers (high clouds only) were compared on one plot (Fig. 3.3). NESS had the highest correlations, while Wisconsin had the lowest at the same distance. The Meteosat (ESA) and Japanese (GMS) correlations fell in between. Note that all had correlations of approximately 0.9 at their minimum sampling distance, which was 100 km for Wisconsin and 300 km for NESS. Wisconsin had many observations under 100 km separation. ESA and GMS had few proximate observations and had an effective minimum sampling distance of 100-200 km. NESS cloud motions were even less dense with a mean minimum spacing of approximately 300 km.

Wisconsin may have lower correlations at 400 km and larger distances because of the ±15° latitude restriction. Experiments with limiting the latitude bounds of the high density Seasat data produced a similar decrease in the autocorrelation statistic.

Differences among wind producers are apparent in the directional difference information. Wisconsin had the highest directional differences and NESS the lowest. The speed standard deviations showed the opposite ranking -- Wisconsin and GMS were lower, NESS and ESA higher. These statistics suggest that NESS generated a more directionally smooth product with larger speed variation than Wisconsin.

4. Conclusions

In Section 2, monthly low level wind fields from ship data, from cloud motions and from the GLAS model were compared. The three fields were highly correlated (0.82 to 0.94), with u-components more highly correlated than v-components. There was a 1.2 - 1.4 m/s easterly bias of cloud motions relative to the other two data fields. This is largely attributable to altitude differences. The root mean square differences over grid points were in the range 1.0 to 1.6 m/s. As expected, there were large gaps in ship coverage. Glossing over a few detailed differences (possibly due to coastal or orographic effects), it is clear that all three fields converge toward a consistent picture of the surface or low level wind on a montly time scale. Differences among the fields may arise from boundary layer parameterization as well as different observation sets. This aspect deserves more detailed study.

The goal of the World Ocean Circulation Experiment is monthly average wind fields accurate to 0.25 m/s. The analyses made here are obviously not at this level. The cloud and ship analyses differ randomly by 1 m/s per grid point around the mean bias. This indicates that we know the wind field to roughly 1 m/s with one data source. The combination of cloud and ship data should be more accurate, but to what levels of improvement we do not know. Clearly, to approach the 0.25 m/s accuracy level, it would be desirable to use more than two data sources.

In Section 3 we found that cloud motion, RAOB, and automatic aircraft (Airep) data are statistically similar and probably could be handled similarly in analysis schemes except for the special problem of height assignment for cloud motions. The statistical characteristics are similar in both the low and high levels of the atmosphere.

The data that will require either special editing techniques or large averaging or smoothing are the land surface stations, ship reports, and pilot reported Aireps. Land stations and ship reports have problems with low autocorrelations and excessive variance in wind direction. This may be addressed by editing schemes that remove data with large deviations from the mean. Their speed data had standard deviations equivalent to the other systems, but it was poorly correlated, implying that smoothing is needed. Pilot reports had excessively large standard deviations of scalar speed which implies that special editing and smoothing techniques should be developed specifically for these data.

Some data should not be analyzed with a weighting function extending beyond 300 km because they were poorly correlated at these and longer distances. This is most evident for land surface stations, ship reports, and pilot reported Aireps. These data can provide wind information only in regions where a high density of observations occurs. Averaging a large number of reports is definitely required to remove remnants of very small scale structure.

Although one cannot strictly compare unlike quantities, low level winds appear subjectively to have directional information that is better than their scalar speeds. Their vector correlations were higher than the scalar speeds and the standard deviations of scalar speed showed little increase with distance, except for the Seasat scatterometer data. The flat profile of scalar speed S.D. is especially alarming. It implies that noise, or errors, in the data are as large as the signal or structure in the wind field itself. Accurate analyses would require statistically independent wind speed data in high density to smooth out this noise. In the near future, satellite radar altimeters and passive microwave sensors will be able to produce scalar wind speed information with good coverage for oceans. Because of the deficiency of surface speed information from other sensors, the inclusion of scalar speed data with the conventional wind vector data should be welcomed.

Acknowledgements

The authors are indebted to our librarian, Katherine Gratke, and Robert Williams, NCC, in gathering all of the data from the GWE. Without their efforts, this study would not have been possible. We appreciate the assistance of Dr. Robert Atlas of NASA/GSFC and Mr. James Adleman in giving us the NASA model wind analysis. The Seasat scatterometer data was provided to us by Peter Woiceshyn of the Jet Propulsion Laboratory and Dr. Steven Peteherych of the Atmospheric Environment Service of Canada. We thank them and their institutions for making these data available to us.

This research was funded by Grant NAG5-301 of NASA. Extensive use was made of data obtained under Grant ATM-81-19895 of NSF.

8/DW8/01

List of Figures

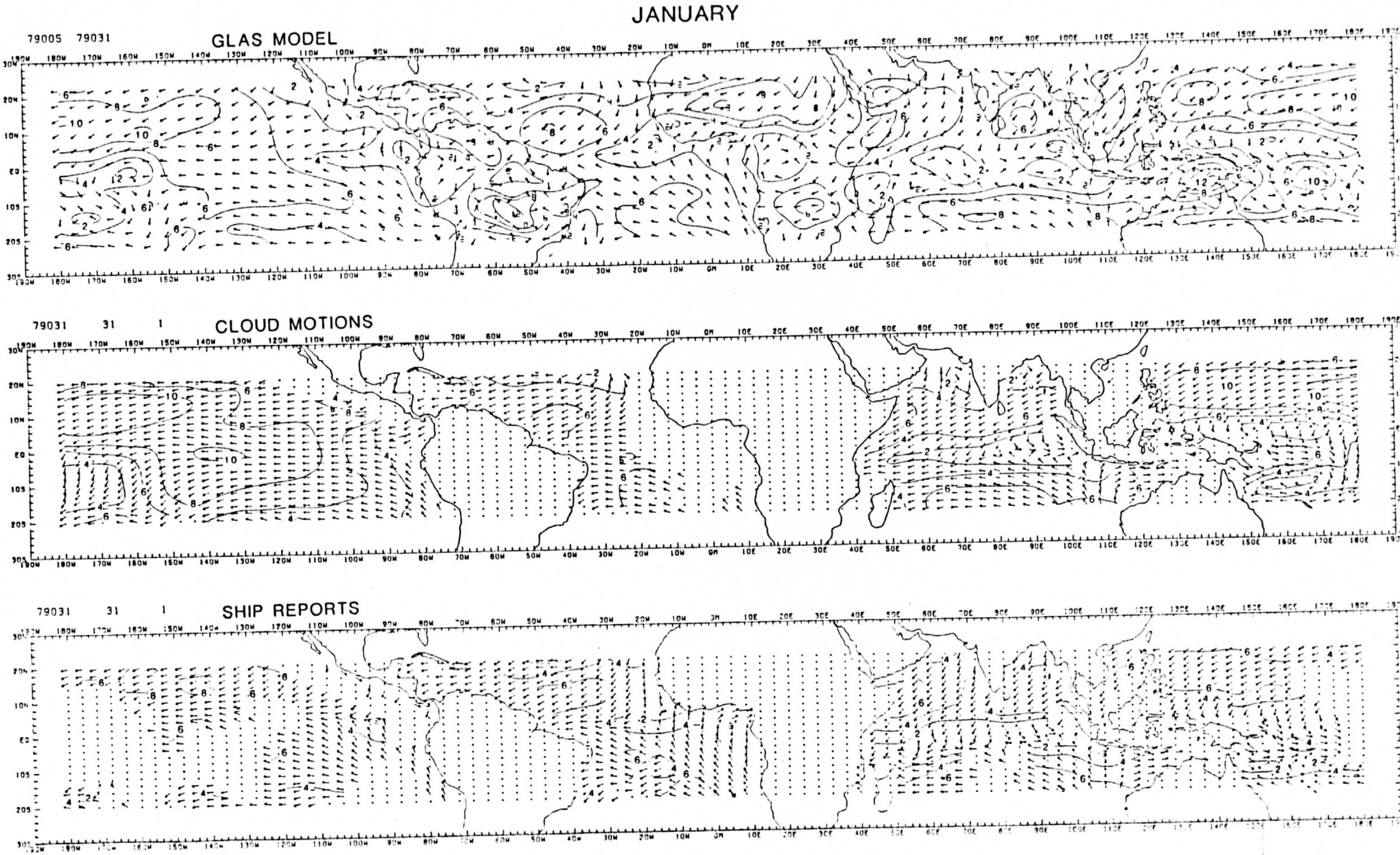

Figure 2.1 January 1979 mean wind fields for the GLAS model averaged from 5-31 January, the low level cloud motions from five geostationary satellites averaged from 1-31 January, and the merchant ship reports (1-31 January). The 944 mb level for the GLAS model was used while all cloud motion reports from 700 mb to the surface (800 mb-sfc for Wisconsin) were used.

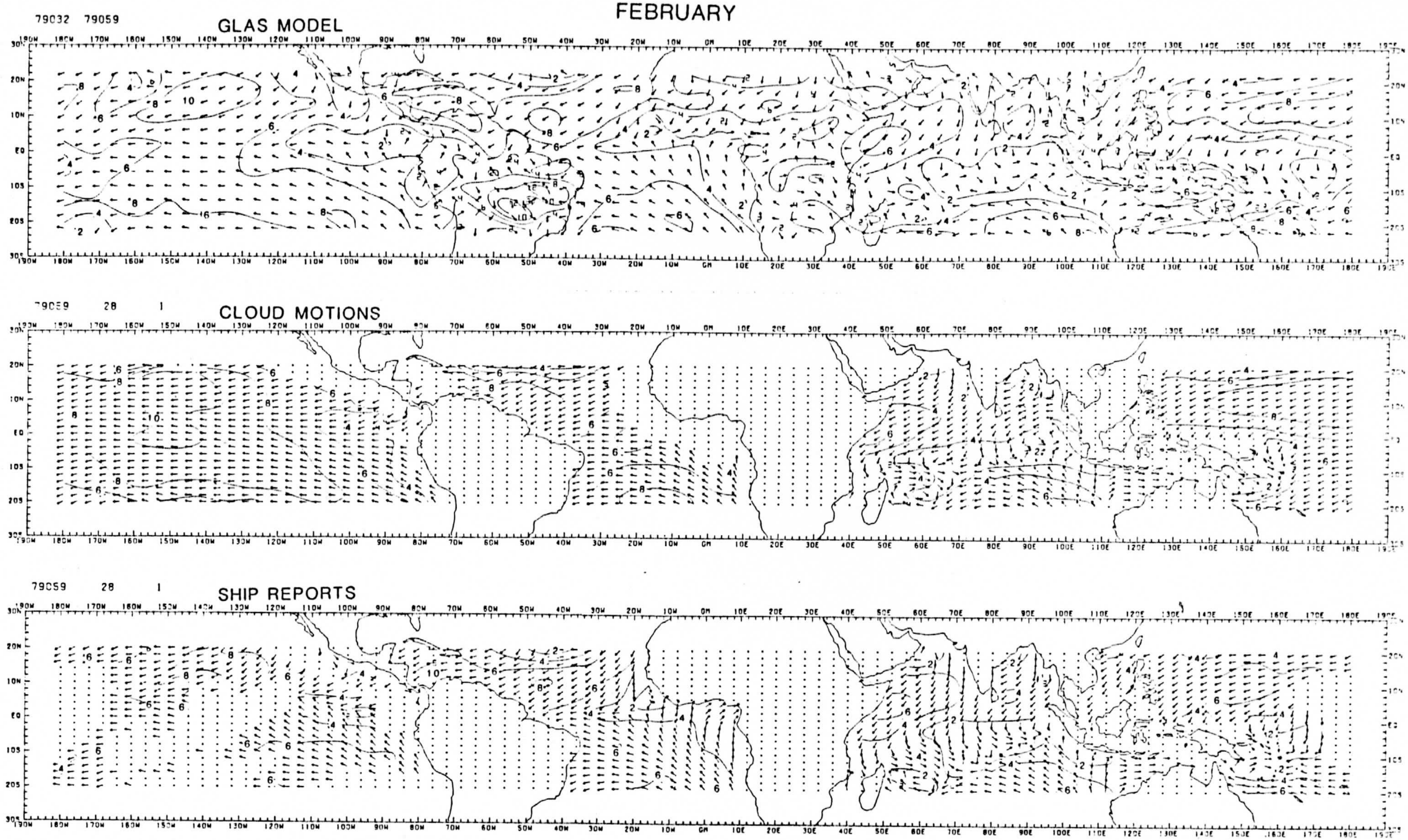

Figure 2.2 February 1979 mean wind fields (1-28 Feb for all data) for the GLAS model 944 mb level, low level cloud motions, and the merchant ship reports.

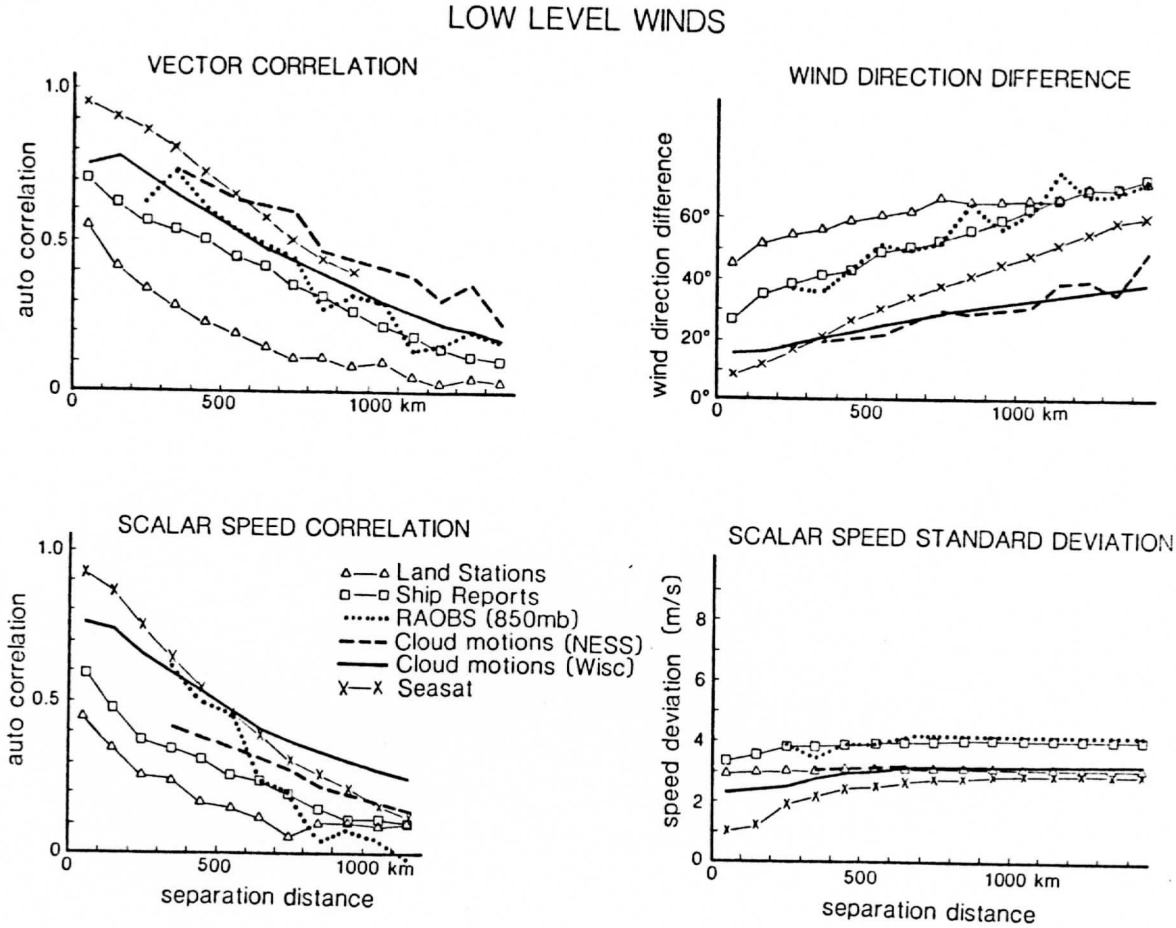

Figure 3.1 The autocorrelations and co-variance statistics for low level wind observations. The vector correlation is defined in Section 3. Co-variance statistics are presented as the standard deviation of the scalar wind speed and the absolute value of the wind direction differences between paired observations.

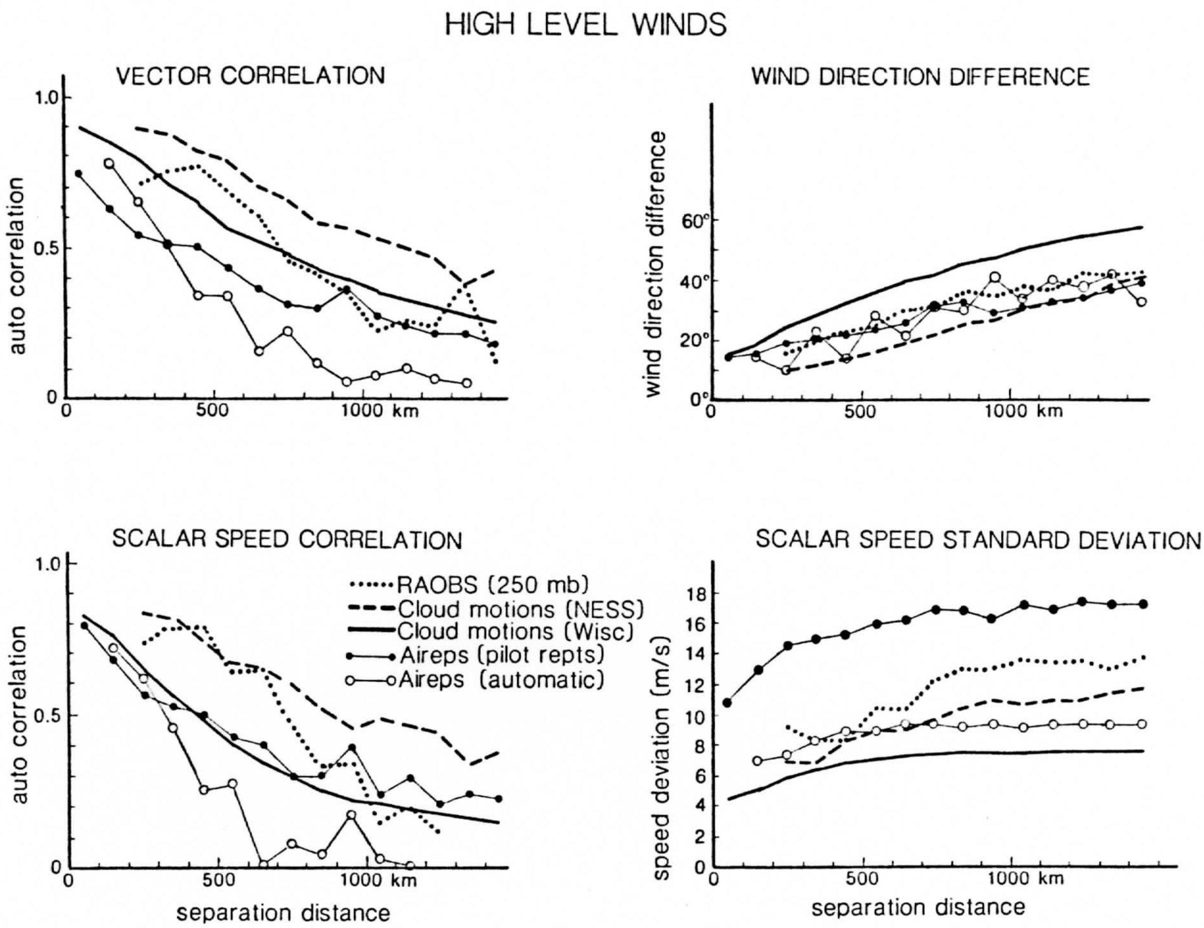

Figure 3.2 The autocorrelation and co-variance statistics of high level wind data. See Section 3 for definition of the statistics.

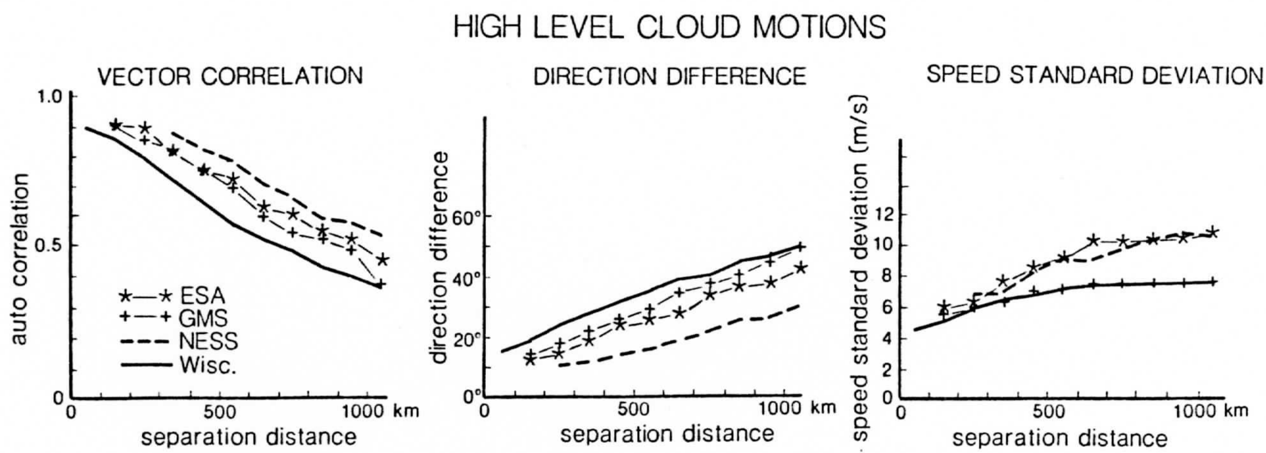

Figure 3.3 The autocorrelation and co-variance statistics for cloud motion data from four different data systems used in the Global Weather Experiment. See Section 3 for definition of the statistics.

References

Baker, W.E., 1983: Objective analysis and assimilation of observational data from FGGE. Mon. Wea. Rev. 111, 328-342

Barnes, S.L., 1964: A technique for maximizing details in numerical weather map analysis. J. Appl. Meteor. 3, 396-409.

Halpern, D. and R.A. Knox, 1983: Coherence between low-level cloud motion vectors and surface wind measurements near 0°, 152°W from April 1979 to February 1980. Atmosphere-Ocean 21, 82-93.

Hasler, A.F., W.C. Skillman, W.E. Shenk, and J. Steranka, 1979: In situ aircraft verification of the quality of satellite cloud winds over oceanic regions. J. Appl. Meteor. 18, 1481-1489.

Hubert, L.F., and L.F. Whitney Jr., 1971: Wind estimation from geostationary satellite pictures. Mon. Wea. Rev. 99, 665-672.

Jones, W.L., L.C. Schroeder, D.H. Boggs, E.M. Bracalente, R.A. Brown, G.J. Dome, W.J. Pierson, and F.J. Wentz, 1982: The Seasat-A satellite scatterometer: The geophysical evaluation of remotely sensed wind vectors over the ocean. J. Geophys. Res. 87, 3297-3317.

Mosher, F.R., 1981: Compatibility of cloud tracked winds from United States, European, and Japanese geostationary satellites. Advances in Space Res. vol 1, 139-146.

Panofsky, H.A. and G.W. Brier, 1968: Some Applications of Statistics to Meteorology, Penn State University Press, College Park, PA, 224 pp.

Pierson, W.J., S. Peteherych, and J. Wilkerson, 1980: The winds of the comparison data set for the Seasat Gulf of Alaska Experiment. IEEE J. of Oceanic Eng. OE-5, 169-176.

Sparkman, J.K., J. Giraytajs, and G.J. Schmidt, 1981: ASDAR: A FGGE real-time data collection system. Bull. Amer. Meteor. Soc. 62, 394-399.

Steinitz, G., A. Huss, A. Manes, R. Sinai, and Z. Alperson, 1971: Optimum station network in the tropics. J. Appl. Met. 10, 364-369.

Wurtele, M.G., P.M. Woiceshyn, S. Peteherych, M. Borowski, and W.S. Appley, 1982: Wind direction alias removal studies of Seasat scatterometer-derived wind fields. J. Geophys. Res. 87, 3365-3377.

Wylie, D.P. and B.B. Hinton, 1981a: Some statistical characteristics of cloud motion winds measured over the Indian Ocean during the summer monsoon. Mon. Wea. Rev. 109, 1810-1812.

Wylie, D.P. and B.B. Hinton, 1981b: The feasibility of estimating large-scale surface wind fields for the summer MONEX using cloud motion and ship data. Bound. Layer Meteor. 21, 357-367.

Wylie, D.P. and B.B. Hinton, 1984: A summary of the wind data available from satellites from the past history to future sensors. Large-Scale Oceanographic Experiments and Satellites, NATO Research Workshop, Riedel Press, Dordrecht, Holland and Boston, U.S.A.; also summarized in the Tropical Ocean-Atmosphere Newsletter, January 1984, published by NOAA Pacific Marine Environmental Lab, Seattle, WA.